Polymer 227 (2021) 123852

Contents lists available at ScienceDirect

Polymer

journal homepage: www.elsevier.com/locate/polymer

Enhancement of crystallization kinetics of poly(L-lactic acid) by grafting with optically pure branches

Alessandra Longo [a,b], Giovanni Dal Poggetto [a], Mario Malinconico [a], Paola Laurienzo [a,**], Ernesto Di Maio [b], Maria Laura Di Lorenzo [a,*]

[a] National Research Council (CNR), Institute of Polymers, Composites and Biomaterials (IPCB), C/o Comprensorio Olivetti, Via Campi Flegrei 34, 80078, Pozzuoli, Italy
[b] University of Naples Federico II, Dipartimento di Ingegneria Chimica, Dei Materiali e Della Produzione Industriale, Naples, 80125, Italy

ARTICLE INFO

Keywords:
poly(L-lactic acid)
Crystallization
Graft copolymer

ABSTRACT

This work details the first example of enhancement of crystallization rate of poly (L-lactic acid) (PLLA) by introducing optically pure short chain branches. A biobased PLLA copolymer was prepared by initial radical functionalization of commercial PLLA with itaconic anhydride (IAH) in a Brabender mixer, then by reaction with a tailor-made hydroxyl-terminated, optically pure PLLA with molar mass $M_n = 4$ kDa, the latter prepared via ring opening polymerization. Gel permeation chromatography and infrared spectroscopy proved the efficiency of grafting reaction, with the amount of grafted IAH quantified via UV–Vis. The synthesized graft copolymer displays faster crystallization rate with respect not only to the commercial grade, but also to a binary blend with the same nominal composition. The role played by the short branches in favoring both crystal nucleation and growth was discussed in terms of molecular nucleation. The results detailed in this manuscript demonstrate that synthesis of a graft copolymer with optically pure short branches is an efficient way to improve the poor crystallization kinetics of PLLA, which is one of the major drawbacks of this polymer.

1. Introduction

Poly (L-lactic acid) (PLLA) is the most extensively studied and used biodegradable and renewable thermoplastic polyester, due to its potential to replace oil-based polymers [1,2]. PLLA is produced by ring-opening polymerization of lactide, the cyclic dimer of lactic acid (LA) [3–5]. The latter, 2-hydroxypropanoic acid, CH_3–CH(OH)–COOH, was discovered in sour milk in 1780 [4]. LA has an asymmetric carbon atom, hence two optically active forms called L-lactic acid (L-LA) and D-lactic acid (D-LA). Commercial PLLA grades are produced from a mixture of both isomers, most commonly containing 96–98% of L-isomer. The presence of both L-LA and D-LA segments in the polymer chain makes PLLA a random copolymer, hence its properties are largely affected by the co-unit content [6–8].

LA can be produced either from petrochemical resources or from annually renewable feedstocks. The first process involves hydrolysis of lactonitrile, a byproduct of acrylonitrile production, and results in a racemic L-LA/D-LA mixture, which is a severe weakness [9]. The second process relies on microbial fermentation and can generate almost optically pure L-LA or D-LA [4]. This process has a number of additional advantages, namely the use of renewable carbohydrate biomass as feedstock, and low energy consumption due to low temperature processing. For these reasons, almost all lactic acid produced globally derives from microbial fermentation technology.

Despite the several favorable properties, PLLA has a few drawbacks that have limited so far a wider commercial exploitation. The slow crystallization kinetics is probably the major weak point of PLLA, as it hampers the attainment of degrees of crystallinity suitable for mechanical, thermal and transport properties, among others, required in several commercial products [1,2]. It also affects foaming, with PLLA foams being of large industrial interest for biological and medical applications (e.g., tissue engineering and medical implant materials) [10–13]. As typical for random copolymers, chain composition largely affects crystallization kinetics of PLLA, which becomes increasingly slower with the decrease of stereoregularity of the polymer chain [7,14–16]. However, the high cost of purification of the monomer limits production of highly stereoregular PLLA [4,5], i.e. of a faster crystallizing polymer.

* Corresponding author.
** Corresponding author.
E-mail addresses: paola.laurienzo@ipcb.cnr.it (P. Laurienzo), dilorenzo@ipcb.cnr.it (M.L. Di Lorenzo).

https://doi.org/10.1016/j.polymer.2021.123852
Received 23 January 2021; Received in revised form 30 April 2021; Accepted 5 May 2021
Available online 10 May 2021

Huge research efforts have been devoted in the latest two decades to improve crystallization kinetics of PLLA. Major successful routes include variation of formulation, eg. by the addition of nucleating agents and/or plasticizers, and a tailored chain structure, which may involve branched or multi-arm architectures that also largely affects processing and foaming behavior.

Several literature reports indicate that long-chain branching (LCB) has a significant effect on polymer crystallization, and that a small amount of LCB can increase the number of nucleus sites, resulting in a higher rate of crystallization [17–20]. In the case of PLLA, both an enhancement and a diminution of crystallization rate have been observed, determined by the degree of branching and the branch length [20–27]. The branching points, which can be regarded as a point of intersegmental connection, as well as chain directional change at branching points, are also expected to disturb the segmental mobility for the nuclei formation and/or the growth of crystallites [26], and there is a critical degree of LCB below which crystallization rate of PLLA can be enhanced [25].

Blending with oligomeric PLLA can lead to a faster crystallization rate, as it results in an enhanced chain mobility due to a decrease of the glass transition temperature (T_g) [28,29]. Tailored blending of a poorly stereoregular, high molar mass polymer with a low molar mass one produced from pure L-LA, can exploit both favorable effects of blending with low molar mass component, and its faster crystallization rate. In fact, a marked improvement of crystallization rate was demonstrated by blending a typical commercial PLLA, with high molar mass (120 kDa) and containing 4% of D-isomer, with a PLLA grade of high stereoregularity, made of pure L-isomer, and a much lower molar mass of 4 kDa [30]. Both crystal growth rates and nucleation kinetics were sizably improved. The faster nucleation rate was ascribed to the easier crystallization of the regular oligomers, which start to crystallize at higher temperature than the commercial grade, and act as nuclei for the subsequent crystal growth that involves both blend components [30].

As mentioned above, chain branching can also have positive effects on crystallization rate, but, to our knowledge, the effects of branching on crystallization rate of PLLA has been investigated only for polymers where the branches and the main chain have the same L-LA/D-LA ratio. It may be possible that branches made of optically pure L-LA can enhance crystallization rate of a poorly stereoregular grade with high molar mass, similarly as found for the blends.

In order to compare the effect of a varied chain structure with the effect of blending, a branched PLLA was prepared using the same PLLA commercial grade of Ref. [30] as main chain, i.e. a high molar mass polymer containing 4% D-isomer, with side branches made of pure L-LA of the same molar mass of the diluent used in Ref. [30]. The graft copolymer was prepared by initial functionalization of PLLA with itaconic anhydride (IAH), followed by reaction of grafted anhydride groups with a tailor-made hydroxyl-terminated, optically pure PLLA, with molar mass M_n = 4 kDa ($PLLA_{4k}$). Itaconic anhydride was preferred to the most commonly used maleic anhydride (MAH) [31–33], not only because the C=C double bond located out of the anhydride ring makes IAH more reactive than MAH towards radical grafting, but also because IAH can be derived from renewable resources, hence the resulting graft copolymer remains fully bio-based [34,35].

Details of polymer synthesis and characterization are presented below, together with analysis of crystallization kinetics. Crystal growth and overall crystallization rates are compared to the neat polymer, as well as to a blend made of commercial PLLA containing 4 wt% of D-isomer, and optically pure PLLA with molar mass M_n = 4 kDa, where the blend has the same nominal composition of the graft copolymer. The aim is to define the effects of chain architecture, apart from the influence of the same pendant groups on crystallization kinetics of PLLA.

2. Experimental part

2.1. Materials

A commercial PLLA grade (c-PLLA) with L-isomer content of 96% and melt-flow index of 6 g/10 min (210 °C/2.16 kg), grade name PLA Lx175 [36] was kindly provided by Total Corbion (The Netherlands). Before processing, the polymer was dried in a vacuum oven overnight at a temperature of 60 °C to remove excess of moisture and avoid degradation. Pure L-lactide (LLA), also kindly provided by Total Corbion (The Netherlands), was dried, prior to use, under high vacuum in presence of P_2O_5 for 20 h. Chloroform, dichloromethane, ethanol, acetone, diethyl ether, and 1,2-dichlorobenzene were purchased from Romil as HPLC grade. Itaconic anhydride (IAH), Luperox 101 (L_{101}), tin (II) 2-ethylexanoate ($Sn(Oct)_2$), sodium hydride (NaH) and Disperse Red 1 (DR1) were purchased from Sigma Aldrich and used without further purifications. 1-decanol (Sigma Aldrich) was dried for 20 h over molecular sieves 3 Å before use.

2.2. Synthesis of PLLA-g-$PLLA_{4k}$ copolymer

2.2.1. Synthesis of hydroxyl-terminated PLLA with molar mass 4 kDa

Hydroxyl-terminated PLLA with molar mass 4 kDa ($PLLA_{4k}$) was synthesized by ring-opening polymerization using L-lactide as monomer, $Sn(Oct)_2$ as catalyst and 1-decanol as initiator. Based on literature data [3–5], the monomer to initiator ratio was set at 27.75, with the aim to obtain a value of M_n around 4 kDa.

In a round bottom flask, 10.09 g (0.07 mol) of LLA were charged. After monomer melting, the initiator (0.4 g, 0.0025 mol) and then the catalyst (760 μL) were added and the reaction was carried out for 24 h at 120 °C under argon atmosphere. The product was solubilized in 15 mL of chloroform and precipitated in a large excess of ice cold diethyl ether. The final polymer was filtered and dried under vacuum overnight. (yield = 88%).

^{1}H NMR: 0.88 ppm (-$CH_{3\,decanol}$, t, 3H),1.27 ppm (-$CH_{2\,decanol}$, m, 14H),1.58 ppm (-$CH_{3\,PLLA}$, d, 168H), 4.35 ppm (-C**H**-$OH_{PLLA\,term}$, q, 1H), 5.17 ppm (-CH_{PLLA}, q, 56H). M_n evaluated by NMR = 4.104 kDa.

2.2.2. Functionalization of PLLA with itaconic anhydride by radical grafting

In order to prepare copolymers with controlled grafting degree, c-PLLA was functionalized with IAH [33,35]. Reaction was performed using a Brabender-like apparatus Rheocord EC of Haake Inc. (Vreden, Germany), using 98.7 wt% of c-PLLA, 0.8 wt% of IAH, and 0.5 wt% of peroxide L_{101}.

The reaction was carried out at 190 °C and 30 rpm mixing rate. c-PLLA was loaded and melted for 2 min, then IAH was loaded into the chamber and the mixture was homogenized for 1 min. Lastly, the initiator L_{101} was added and the reaction was carried out during mixing for the next 6 min. The reaction product was purified by dissolving in 1,2-dichlorobenzene (concentration 10 wt %) at 180 °C using a reflux condenser, precipitated in a large excess of ethanol and then washed in ethanol for three times to remove unreacted c-PLLA. The supernatant containing unreacted monomer (IAH) was removed by filtration and the final product was dried overnight at 60 °C under vacuum.

The dried product was washed in acetone at room temperature for 48 h to selectively remove low molar mass degradation products and residues of unreacted IAH. The solvent was removed after sedimentation and the purified product (PLLA-IAH) was dried under vacuum and used for further characterization and branching reaction.

2.2.3. Coupling reaction of $PLLA_{4k}$ with PLLA-IAH

PLLA-IAH (1.00 g, corresponding to $4.90 \cdot 10^{-5}$ mol of IAH) was dissolved with dry dichloromethane (25 mL) in a round bottom flask at 60 °C under argon atmosphere. A solution of $PLLA_{4k}$ (0.27 g, $5.13 \cdot 10^{-5}$ mol) in 15 mL of dichloromethane containing 0.0012 g ($5.13 \cdot 10^{-5}$ mol)

of NaH (corresponding to a molar ratio $PLLA_{4k}$/NaH = 1/1) was prepared separately, and maintained under continuous stirring at room temperature until hydrogen bubbling stopped (around 20 min). The two solutions were then merged and stirred under argon stream at 60 °C overnight. The mass ratio between PLLA-IAH and $PLLA_{4k}$ corresponds to 80/20 w/w. The final solution containing the crude product was first centrifuged to remove insoluble impurities, then concentrated by rotavapor and finally poured in cold hexane to precipitate the product (yield = 90%).

To estimate the mass of unreacted $PLLA_{4k}$, and to remove any other side reaction product involving degradation of polymers, the final product was dissolved in chloroform and dialyzed in a dialysis membrane (cut-off 12 kDa) against chloroform for 48 h to ensure a complete extraction. Then the dialysis membrane was removed and the washing chloroform containing unreacted $PLLA_{4k}$ and any side reaction product was evaporated by rotavapor. The amount of the recovered residue was weighed and found less than 1% wt of total initial mass, indicating the high efficiency of the reaction and absence of side and degradation reactions.

2.3. NMR analysis

^{1}H and ^{13}C NMR spectra were recorded on a 600-MHz Bruker AVANCE-III Spectrometer (Bruker BioSpin GmbH, Rheinstetten, Germany). Sample concentrations were about 0.7% (w/v) in $CDCl_3$.

2.4. Gel permeation chromatography

Gel permeation chromatography (GPC) analysis was performed with a GPC Max Viscotek equipped with a Malvern TDA with refractive index (RI), right angle laser light scattering (RALS), low angle laser light scattering (LALS) and intrinsic viscosity (*IV*) detectors. Samples were dissolved and eluted in $CHCl_3$ (Romil) at flux of 0.8 ml min^{-1}, with injection volume of 100 μl, concentration of 5 mg $ml^{-1}$and analyzed through a column set composed by a precolumn and two columns Phenogel Phenomenex, with exclusion limits 10^6 and 10^3 Da.

All samples were evaluated with triple point calibration (polystyrene standard M_n = 101.252 kDa and M_w = 104.959 kDa).

GPC OmniSEC software allows to evaluate the weight average number of branches per macromolecule (B_n) of a polydisperse sample and the branching frequency (λ) considering c-PLLA as linear reference. B_n is calculated starting from Eq. (1)

$$g' = \frac{[\eta]_b}{[\eta]_l} \tag{1}$$

where *g*' is the intrinsic viscosity contraction factor and $[\eta]_b$ and $[\eta]_l$ are the intrinsic viscosities of branched and linear samples, respectively. The parameter *g*' is correlated to the radius of gyration contraction factor (*g*) by the following equation (Eq. (2))

$$g' = g^{\varepsilon} \tag{2}$$

where ε is the shape factor, which is taken to be 0.75 [37].

The relation between the number of branches per molecule B_n and the contraction factor is described by the following Zimm–Stockmayer equation (Eq. (3)) [37].

$$g = \frac{6}{Bn}\left\{\frac{1}{2}\left(\frac{2+Bn}{Bn}\right)^{\frac{1}{2}} \ln\left[\frac{(2+Bn)^{\frac{1}{2}} + Bn^{\frac{1}{2}}}{(2+Bn)^{\frac{1}{2}} - Bn^{\frac{1}{2}}}\right] - 1\right\} \tag{3}$$

The branching frequency (λ) is calculated as follows (Eq. (4)):

$$\lambda = 100R\frac{Bn}{Mw} \tag{4}$$

where *R* is the molecular weight of the repeating unit (72 Da) and M_w is the molecular weight of the polymer.

2.5. Fourier Transform Infrared Spectroscopy

Functional groups characteristics of PLLA-IAH were observed via Fourier Transform Infrared Spectroscopy (FTIR), using a PerkinElmer FTIR Spectrometer Model Spectrum 100, in reflection mode. The instrument is equipped with a PerkinElmer Universal Attenuated Total Reflectance (ATR) sampling accessory with a diamond crystal. Each spectrum was determined as average of 16 individual scans, each one recorded at a resolution of 4 cm^{-1}. Chloroform was used as solvent to prepare cast films for FTIR-ATR analyses.

2.6. UV–vis spectroscopy

The effective amount of IAH grafted on PLLA chains was quantified via UV–Vis analysis. UV–Vis absorption spectra were recorded in the 200–800 nm range, at a 0.5 nm/s scan rate, using a Jasco UV–Vis spectrophotometer Mod. V570. DR1was used as chromophore.

The chromophore solution was prepared by dissolving 0.07 g of DR1 in chloroform, then stoichiometric amount of NaH was added to deprotonate DR1. Once bubbling of hydrogen stopped, this solution was mixed with 1 g of PLLA-IAH in 25 ml of chloroform and the reaction was carried out for three days. The product, named PLLA-IAH-DR1, was precipitated and washed several times in cold diethyl ether until the UV–vis spectrum of the washing solution showed no more presence of dye, then vacuum dried for 24 h at room temperature. Absorbance was measured for a solution with a concentration of 6 * 10^{-5} M (20 mg/mL) of PLLA-IAH-DR1, and compared with a solution at the same concentration of DR1 in chloroform. The amount of IAH grafted onto the polymer backbone was determined by means of Lambert-Beer equation:

$$A = \varepsilon\, b\, c \tag{5}$$

where *A* is absorbance at 475 nm, ε is the molar absorption coefficient of DR1, *b* is the molar path that amounts to 1 cm in the specific configuration used, and *c* is the molar concentration of the solution. Molar absorption coefficient of DR1 was determined by measuring the absorbance of solutions at different concentration, attained by progressive dilution of a DR1/$CHCl_3$ solution with initial molar concentration of $5 \cdot 10^{-4}$ M (0.16 mg/ml). Interpolating the absorbance values corresponding to the maximum of the absorption peak of DR1 at 475 nm, a molar absorption coefficient of DR1 in chloroform was calculated as ε = 8.03 L $mol^{-1}cm^{-1}$.

2.7. Preparation of PLLA-IAH/$PLLA_{4k}$ blends

Binary blends with the same nominal composition of the branched polymer were prepared by solution casting using chloroform (0.04 g/mL), to attain films with a thickness of about 200 μm. Once the solvent was evaporated, the samples were further dried under vacuum for 24 h.

2.8. Thermal analysis

Thermal properties of the samples were investigated using a PerkinElmer Pyris Diamond DSC, equipped with an Intracooler II as cooling system. Temperature and energy calibration was performed with a high purity indium standard.

To analyze isothermal crystallization kinetics, the samples were melted at 200 °C for 2 min, then cooled to the desired crystallization temperature (T_c) at 30 K min^{-1}. The same melting conditions were used to investigate non-isothermal crystallization analysis: the various formulations were melted at 200 °C for 2 min, then cooled at 30 K min^{-1} to 160 °C, followed by cooling at 4 K min^{-1} to room temperature. Glass transition was analyzed after melting at 200 °C for 2 min, followed by fast cooling at the programmed rate of 100 K min^{-1} to 0 °C, then heating at 20 K min^{-1}.

Dry nitrogen was fluxed as purge gas at a rate of 30 mL min^{-1}. A fresh

specimen was used for each analysis. All the experiments were repeated three times to ensure reproducibility.

2.9. Optical microscopy

A Zeiss Axioskop polarized-light optical microscopy (POM) and a Linkam THMS 600 hot stage were used to measure spherulite growth rates. A thin film of each sample (thickness less than 10 μm) was obtained by squeezing between two circular Linkam cover slips on a hot stage and manually pressing. For the analysis of crystallization kinetics, the samples were melted at 200 °C for 2 min, then cooled at 30 K min^{-1} to T_c. Nitrogen gas was fluxed in the Linkam hot stage to limit degradation.

A Scion Corporation CFW-1312C Digital Camera coupled with Image-Pro Plus 7.0 software (Media Cybernetics) was used to capture images at a pre-defined sampling rate. Spherulite radii were plotted as a function of time to obtain spherulite growth rates by linear fitting.

3. Results and discussion

3.1. Synthesis and characterization of PLLA-g-$PLLA_{4k}$ copolymer

Functionalized PLLA can be prepared following two main strategies: ring opening polymerization (ROP) of selectively modified lactides, or post-polymerization modification [3–5]. The latter consists in preparation of new materials through modification of pre-synthetized polymer precursors, and is preferred as it allows to characterize the initial polymer before functionalization and to tune the degree of modification. In this work, a graft PLLA copolymer of predefined structure and composition was synthetized in two steps: in the first step a functional group (IAH) was introduced along the main chain of c-PLLA through radical grafting, and in the second step a pre-synthetized $PLLA_{4k}$ was covalently bonded as side branches by nucleophilic attack of the terminal hydroxyl of $PLLA_{4k,}$ previously activated with sodium hydride [38], to the β-carbonyl of anhydride, which has less steric hindrance. The synthetic route is illustrated in Fig. 1.

In the first step, the radical grafting of IAH was performed in a Brabender-like apparatus, operating in mild conditions with low percentages of reactants, in order to limit side reactions and degradation. This was followed by multistep purification, as detailed above, to eliminate all by-products and, in particular, low molar mass PLLA chains [34,35]. Confirmation of successful grafting was obtained by FTIR and GPC, and degree of modification was quantified by UV–Vis as discussed below.

PLLA with molecular weight around 4 kDa was synthesized by classical ROP polymerization of LLA, using 1-decanol as initiator. The molecular weight was controlled by the –OH/LLA molar ratio in the feed and calculated by the ratio between the intensities of the resonance associated with -C**H**–OH proton of PLLA terminal at 4.35 ppm and the resonance of –CH proton of the repeating unit at 5.17 ppm in the NMR spectrum.

The second step concerns the binding of $PLLA_{4k}$ to the carbonyl group of IAH. Due to the purpose of the present work to make a comparison between the effect on crystallization kinetics of chain branching with respect to blending of a low amount of higher stereoregular PLLA [30], the desired amount of $PLLA_{4k}$ branches should not be higher than 20 wt%. Therefore, a PLLA-IAH with low amount of IAH, corresponding to 0.5 wt%, was chosen to obtain the desired branching degree.

Before the second step of synthesis, the amount of IAH grafted on PLLA chains was quantified. To prove the presence of grafted IAH on PLLA chains, PLLA-IAH was analyzed via FTIR-ATR. Unfortunately, most of IAH absorption bands overlap with PLLA ones. Absorption band at 1750 cm^{-1} related to C═O stretching vibrations of cyclic anhydrides is fully hidden under the C═O stretching vibration of PLLA and this,

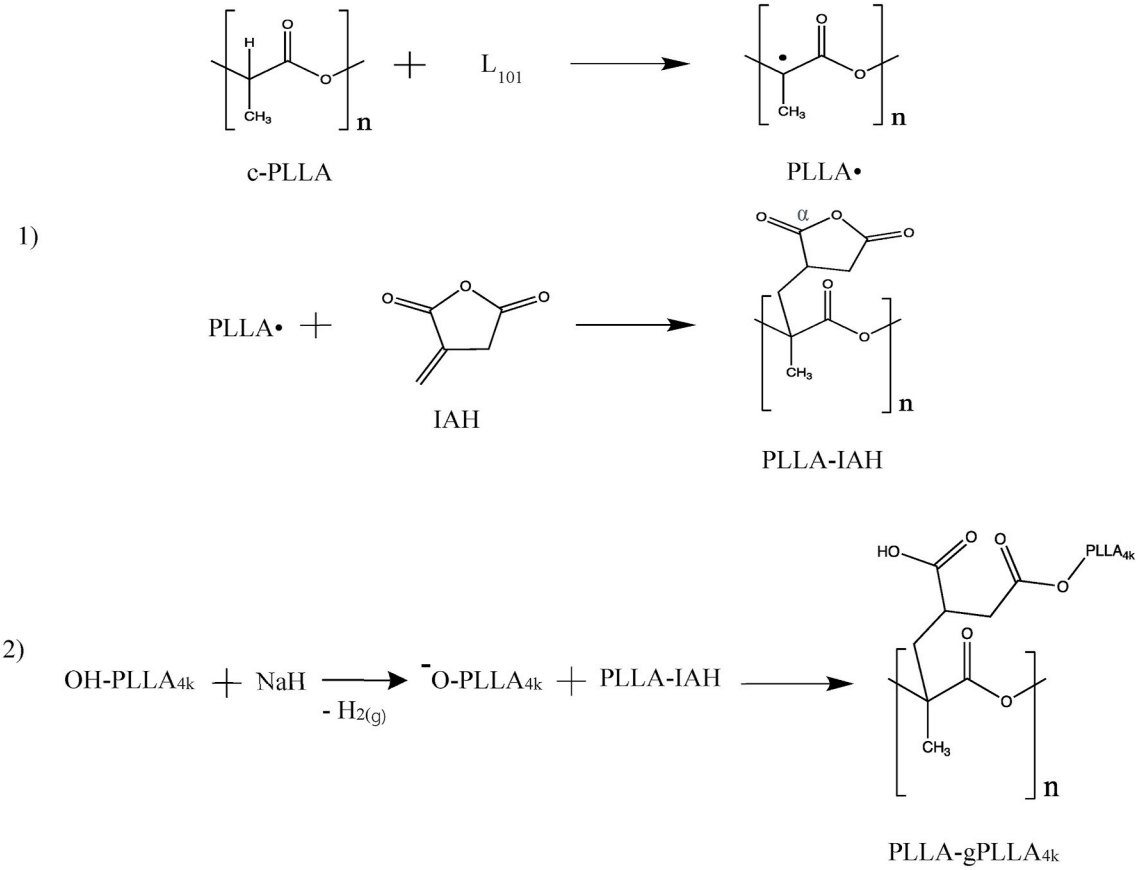

Fig. 1. Synthetic route to PLLA-g-PLLA4k.

together with low concentration of IAH, hampers the use of this band to prove the presence of grafted anhydride.

In order to overcome these problems, it was attempted to normalize both c-PLLA and PLLA-IAH spectra to the band at 1167 cm^{-1} related to the C–C vibrations between CH_3 and tertiary carbon of PLLA backbone. As reported in Ref. [35], where non-reacted PLLA is compared to PLLA containing 5 and 10 wt% IAH, this normalization should allow to detect an increase in the intensity of C═O stretching band from neat c-PLLA to PLLA-IAH. Unfortunately, this variation could not be appreciated in our samples, where concentration of IAH is only 0.5 wt%, too low to show a perceptible difference between the two spectra in analysis, as demonstrated in the insert of Fig. 2.

Focusing on the wavenumber range of 2800–3100 cm^{-1}, FTIR spectrum of PLLA-IAH shows two absorption bands at 2854 and 2925 cm^{-1} which, according to Ref. [35], can be assigned to CH_2– functional groups of the grafted anhydride. Even if these bands are not present in the spectrum of pristine c-PLLA, they cannot uniquely prove the effectiveness of grafting reaction, which could be related also to CH_2– terminal groups generated by a chain scission reaction. However, mild polymerization conditions and a low [L_{101}] have been selected to reduce the chance of side reactions, then purification of PLLA-IAH in acetone for 48 h selectively extracts low molar mass chains, therefore most of any chain scission products are removed in this step. These considerations support the effectiveness of grafting reaction.

Fig. 3a shows the ^{1}H NMR spectra of PLLA-IAH and PLLA-*g*-$PLLA_{4k}$. In both spectra, besides the peaks associated to the main polymer chain [39], the small signal at 2.5 ppm (denoted as "a" in the Figure), absent in PLLA spectrum (not shown), is related to grafted IAH, as it can be attributed to the -C**H$_2$**- of the anhydride ring, generally located in the region 2–3 ppm [33]. Furthermore, the absence of the resonance characteristic of **–**C═C**H$_2$** protons of free anhydride in the range 4.5–5.5 ppm supports the occurrence of chemical grafting of IAH on PLLA chains. In PLLA-*g*-$PLLA_{4k}$ spectrum, three new peaks attributed to grafted $PLLA_{4k}$ are observed at 3.75, 1.27 and 0.88 ppm. The resonance at 3.75 ppm can be assigned to the –CH- proton of the terminal unit of $PLLA_{4k}$ conjugated to IAH (denoted as "b" in the Figure) and is specific to the occurrence of a chemical link between IAH and $PLLA_{4k}$. The peaks at 1.27 and 0.88 ppm are respectively attributed to –CH_2- and –CH_3 protons deriving from 1-decanol used as ROP initiator of $PLLA_{4k}$. ^{13}C NMR analysis of PLLA-g-$PLLA_{4k}$ confirms the occurrence of grafting and coupling reactions. The spectrum (Fig. 3b) shows, besides main chain signals (**C**═O, 169.61 ppm; **C**H, 69.02 ppm; **C**H_3, 16.65 ppm), the peaks relative to carbonyls (e', 169.36 and e, 169.15 ppm) and **C**H–**C**H_2 (d', 66.72, and d, 65.72 ppm) of anhydride, and to aliphatic carbons from 1-decanol in $PLLA_{4k}$ (35-20 ppm range).

All these evidences, together with the absorption bands reported in FTIR spectrum, corroborate the efficiency of grafting and coupling reactions.

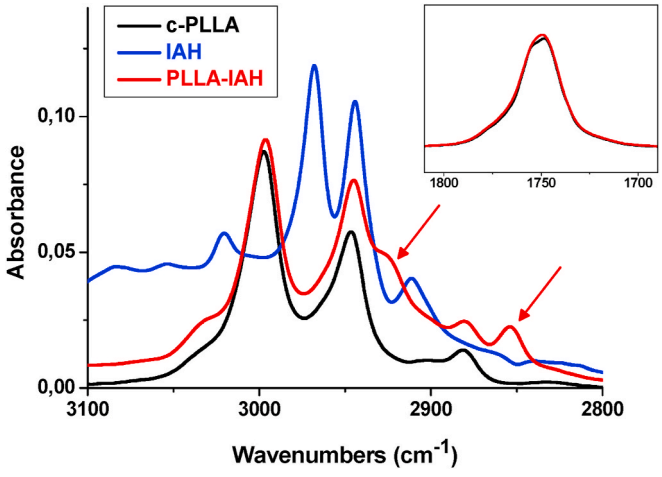

Fig. 2. FTIR spectra of IAH, c-PLLA and PLLA-IAH.

Due to the low intensities of IAH signals, NMR could be not accurate for a reliable quantitative evaluation. *Liu* et al. [40] suggested an alternative method for quantification of grafted anhydride by means of UV–Vis spectroscopy. Thus, in order to determine the functionalization degree, the product was analyzed with UV–Vis spectroscopy, after conjugation of PLLA-IAH with DR1 chromophore. DR1 was chosen for the high solubility and for the presence of a reactive –OH located far from the amino-4-nitroazobenzene chromophoric unit. This feature leads to only negligible variation in terms of λ_{max} after reaction with $PLLA_{4k}$. The reaction scheme is presented in Fig. 4. The reaction was carried out with an excess of chromophore in order to saturate all anhydride groups with DR1. The synthesis pattern is analogous to the one previously described. DR1 was coupled to the carbonyl of anhydride via nucleophilic addition, after activation of the –OH group of DR1 with sodium hydride:

The reaction product was washed several times with diethyl ether, until the UV–Vis spectrum of the washing solution was found free of dye. This purification ensures the separation of unconjugated DR1, thus is possible to assume that the amount of DR1 determined via UV–Vis is conjugated to PLLA-IAH.

UV–Vis absorption spectra of DR1 and PLLA-IAH-DR1 are compared in Fig. 5. Both spectra show the typical absorption band of DR1 in chloroform at wavelength 475 mm, due to interaction between azo functionality (–N═N–) and the attached aromatic moieties [41]. This absorption peak is present both in DR1 and in the PLLA-IAH-DR1 spectra, providing evidence of the effectiveness of grafting reaction. More importantly, it allows to quantify the amount of IAH grafted onto the polymer backbone. The grafting degree of IAH on c-PLLA backbone results to be 0.5 wt%.

Further information on the efficiency of grafting reaction comes from analysis of GPC data, presented in Table 1, which compares weight-average molar mass (M_w), number-average molar mass (M_n), molar mass at peak of the distribution curve (M_p) and intrinsic viscosity (*IV*) of c-PLLA, PLLA-IAH, $PLLA_{4k}$ and PLLA-g-$PLLA_{4k}$. Table 1 shows a sizable decrease of M_n upon addition of IAH to c-PLLA, which suggests some degree of chain degradation occurring upon functionalization reaction concerning mostly low molecular weight fraction of polymer. This behavior is confirmed by a decrease in M_w and by an increase of M_p.

Despite PLLA-*g*-$PLLA_{4k}$ shows higher values of M_w and M_p than c-PLLA, it has a lower *IV* suggesting the presence of branching [42]: the volume occupied by a branched structure is lower than that occupied by a linear structure, which results in a lower *IV* for the branched polymer. GPC data were used to derive Mark-Houwink plots, which relate molar mass to *IV* [43], as presented in Fig. 6. Mark-Houwink equation describes a power law relation between molecular weight and intrinsic viscosity, which is linear in the case of linear polymers. Branched polymers display deviation from linearity related to branching [42], with the deviation increasing with the branching number.

As seen in Fig. 6, the commercial grade (c-PLLA, green curve) shows the highest *IV*, due to the looser conformation in the eluent of the linear polymer (higher hydrodynamic volume) with respect to the modified polymers; grafting with itaconic anhydride (PLLA-IAH, black curve) leads to a slightly lower *IV* in the high M_w range, attributable to some branching arising from radical recombination mechanisms, according to ref. 35. Intrinsic viscosity further decreases upon reaction with $PLLA_{4k}$ (PLLA-g-$PLLA_{4k}$, red curve). Not only PLLA-g-$PLLA_{4k}$ shows the lowest *IV*, but it also displays a more curved downward profile in the high molecular weight range, which is characteristic of branched polymers [42].

Branching leads to an increase in the molecular density of the polymer, which is reversely proportional to *IV*, and the radical grafting is more probable to occur for higher molecular weights. So, increasing the molecular weight, the chance of branching points increases and the differences between linear and branched polymer are more evident.

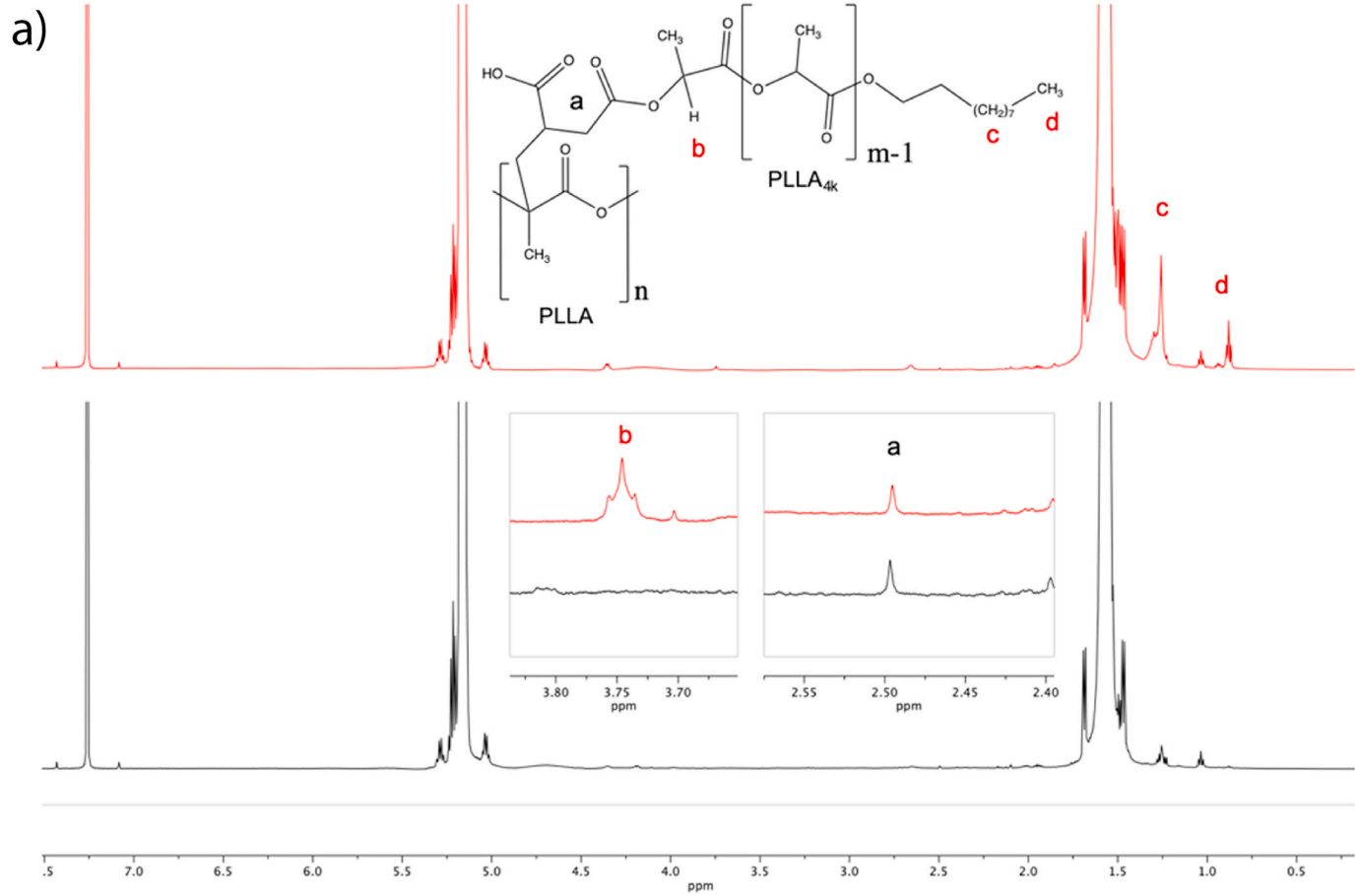

Fig. 3a. ^{1}H NMR spectra of PLLA-IAH (black) and PLLA-*g*-PLLA$_{4k}$ (red). (For interpretation of the references to colour in this figure legend, the reader is referred to the Web version of this article.)

Thus in the high M_w range, the Mark-Houwink line of PLLA-g-PLLA$_{4k}$ curves downward because the sample has a lower hydrodynamic volume due to a more compact conformation in the solvent [42] proving a higher efficiency of grafting reaction in this M_w range. Furthermore, through GPC software it was possible to evaluate the average number of branches per macromolecule (B_n) and the branching frequency (λ) as 11.05 and 0.416, respectively, which correspond to an average value of one branch every 240 repeating units.

3.1.1. *Thermal properties and crystallization kinetics of PLLA-g-PLLA$_{4k}$ copolymer*

From the data reported and discussed above we can reasonably assume that the synthesized PLLA-*g*-PLLA$_{4k}$ sample presents a random distribution of branches made of optically pure PLLA segments, grafted onto a PLLA backbone with lower optical purity. The thermal properties and the crystallization behavior of the synthesized sample were compared to PLLA-IAH, as reference, and to a blend containing the same mass composition of the graft copolymer, i.e., made of 80 wt% of PLLA-IAH and 20 wt% of PLLA$_{4k}$. The latter comparison was performed as an effort to investigate the influence of branched chain architecture on crystallization kinetics. As detailed in Ref. [30], blending c-PLLA with a highly stereoregular PLLA oligomer results in a sizable increase of both nucleation and crystal growth rates. Therefore, any measured variation in crystallization kinetics of the branched polymer may in principle be ascribed the presence of short stereoregular chains, which favor crystallization even if not covalently bonded to the main PLLA chain.

Fig. 7 presents the thermal analysis of these PLLA-based formulations. Data were measured upon heating at 20 K min^{-1}, after cooling at 100 K min^{-1}. PLLA-IAH displays a glass transition (T_g) centered at 61 °C, typical of PLLA [1], coupled to a small enthalpy relaxation endotherm due to the different heating and cooling rates used [44]. Blending PLLA-IAH with OH-terminated PLLA oligomer made of pure L-isomer units (sample coded as "blend") results in a marked decrease of T_g, down to about 55 °C, with a similar decrease in T_g observed also in the PLLA-*g*-PLLA$_{4k}$ graft copolymer (sample coded as "graft"). The measured diminution of T_g in the blend is in line with literature data of PLLA blends with comparable composition, when a high molar mass PLLA is blended with low molar mass grades [29,30], with the latter often added to PLLA formulation as plasticizers [28,45–49]. Similar decreases of T_g have been reported also for branched polymers, compared to linear chains of similar molar mass, and arise from the higher free volume due to the increased number of chain ends in the branched architecture [50–52].

Above T_g, PLLA-IAH displays a broad cold crystallization exotherm, centered around 130 °C, followed by a melting peak at 153 °C. The cold crystallization exotherms of the blended and grafted formulations are markedly anticipated, compared to the linear grade, being centered around 110–112 °C. This is followed by a double melting peak at 150–160 °C, typical of PLLA containing both α′- and α-crystals, or α′-crystals that transform to α-modification upon heating [1,7,8]. The double endotherm is not seen in PLLA-IAH plot, due to the high crystallization temperature that leads to growth of α-crystals [1,7,8]. The initial, qualitative indication of the faster crystallization kinetics of the samples containing short stereoregular sequences is confirmed by the DSC plots measured upon cooling at 4 K min^{-1}, presented in Fig. 8. The blended and grafted formulations display only minor differences in the experimental data, with a sharp crystallization exotherm appearing on cooling. Conversely, the linear polymer shows a broad and weak

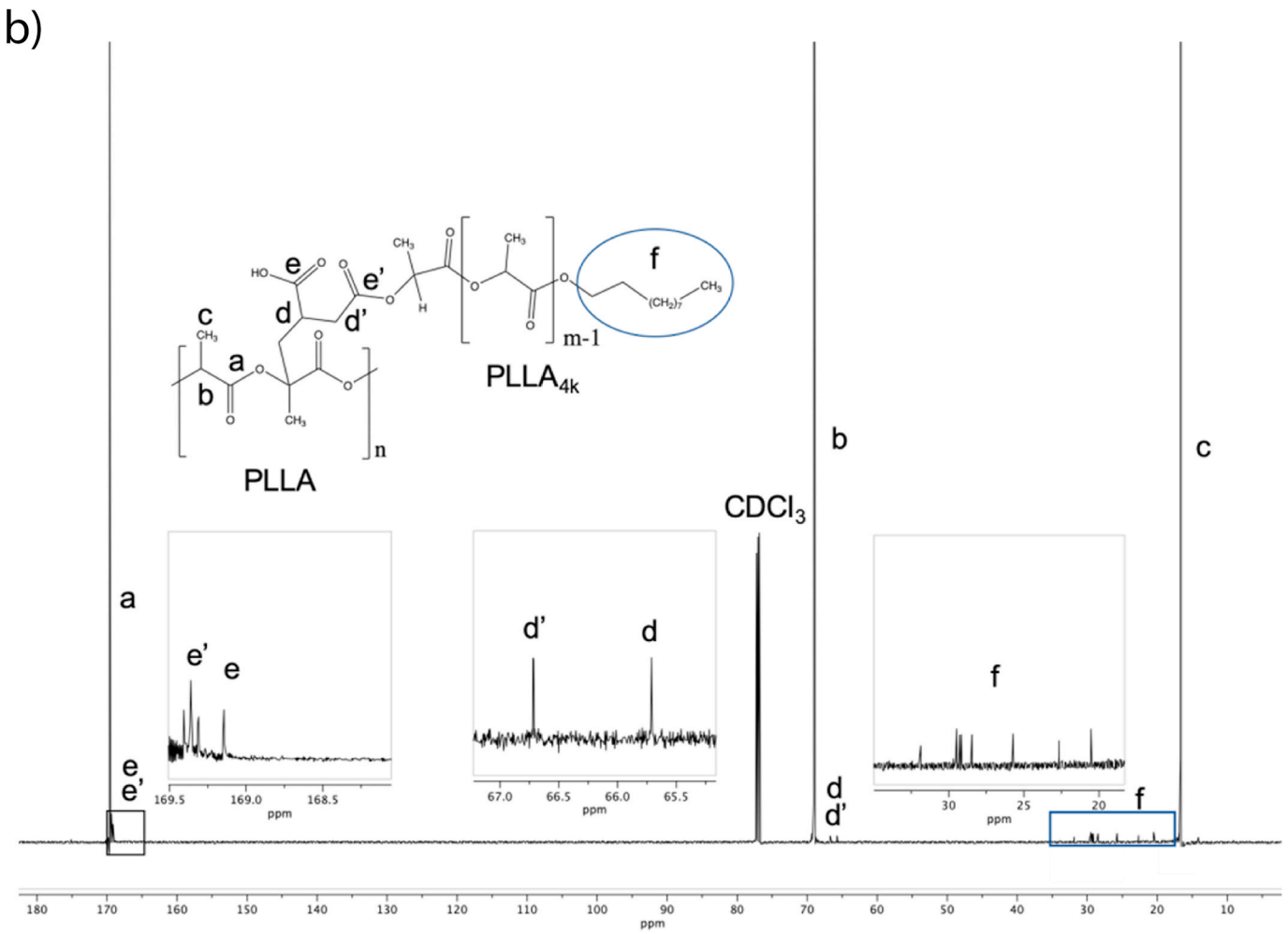

Fig. 3b. ^{13}C NMR spectrum of PLLA-g-$PLLA_{4k}$.

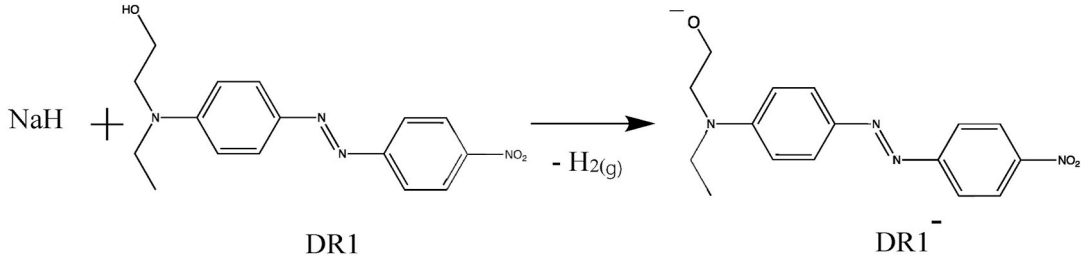

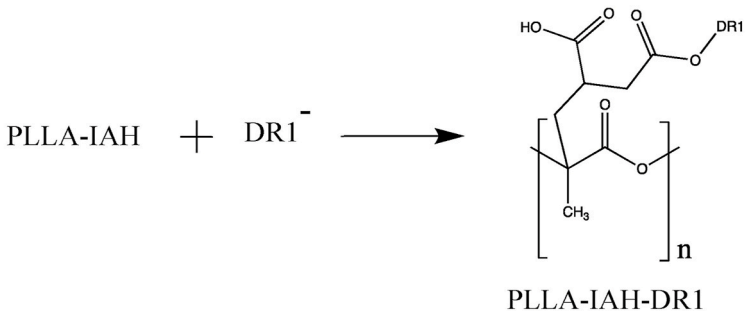

Fig. 4. Synthetic pathway to PLLA-IAH-DR1.

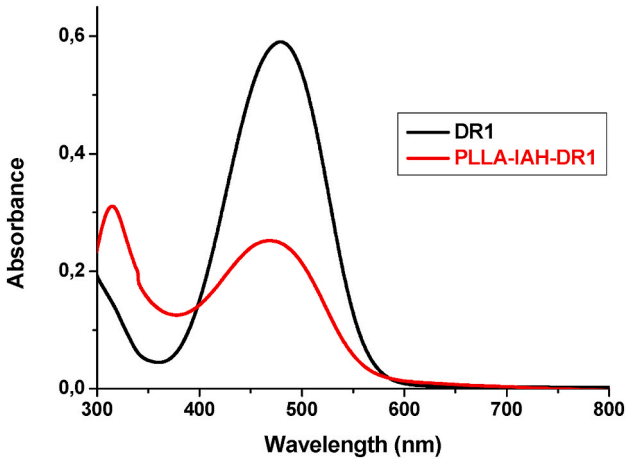

Fig. 5. UV–Vis spectra of PLLA-IAH-DR1 and DR1.

Table 1
Molar mass distribution and intrinsic viscosity of commercial and synthesized samples.

Sample	M_w (kDa)	M_n (kDa)	M_p (kDa)	IV (dL/g)
c-PLLA	104	69	83	1.6
PLLA-IAH	122	33	110	0.75
$PLLA_{4k}$	5.6	4.2	4.9	0.45
PLLA-g-$PLLA_{4k}$	191	52	110	0.54

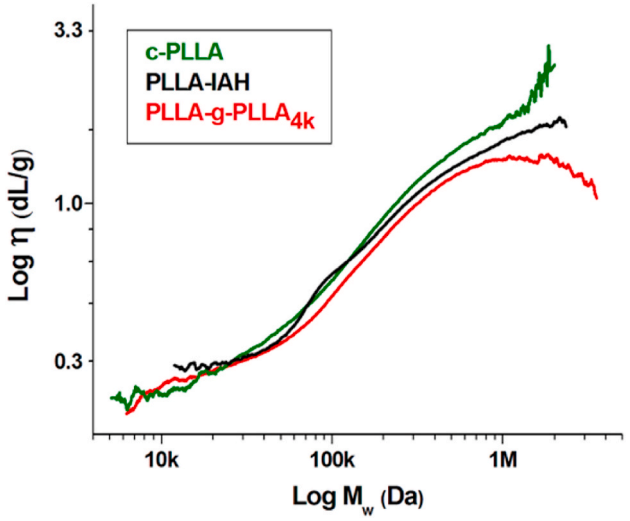

Fig. 6. Mark-Houwink plot of c-PLLA (green), PLLA-IAH (black), PLLA-g-$PLLA_{4k}$ (red). (For interpretation of the references to colour in this figure legend, the reader is referred to the Web version of this article.)

exotherm, which is also delayed compared to the other grades.

Quantitative data on overall crystallization rate of the samples are displayed in Fig. 9, which shows the half-time of crystallization ($\tau_{½}$) as function of the isothermal crystallization temperature (T_c). Data are compared to commercial PLLA, as received (c-PLLA) and melt processed in Brabender mixer (c-$PLLA_{Pr}$). The blended and grafted grades display a much lower crystallization time compared to the plain linear polymer, as well as to the polymer reacted with IAH, indicating their sizable faster crystallization. Data gained for the blended and grafted compositions mostly overlap within experimental uncertainty, with minor differences observed only at temperatures where the crystallization rate is lower.

Comparison of the data presented in Figs. 7–9 reveals that the overall

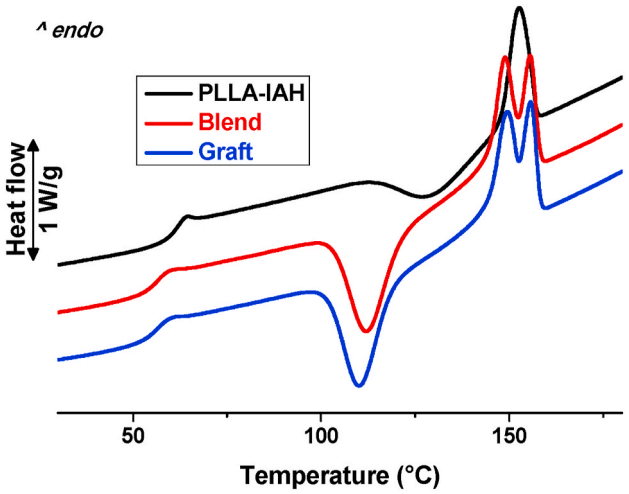

Fig. 7. Heat flow rate plots of PLLA-based formulations, upon heating at 20 K min^{-1}.

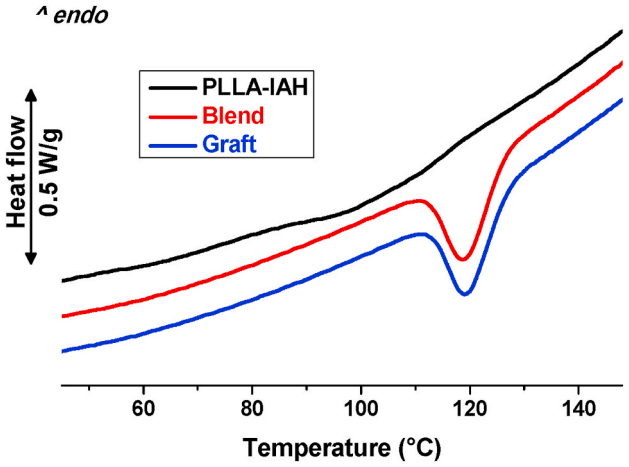

Fig. 8. Heat flow rate plots of PLLA-based formulations, upon cooling at 4 K min^{-1}.

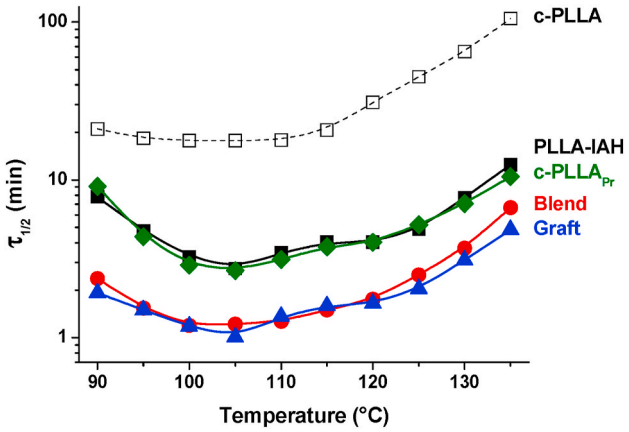

Fig. 9. Half-time of crystallization ($\tau_{½}$) as function of crystallization temperature.

crystallization rate is markedly faster in all the samples, compared to the data reported in Ref. [30], which are also displayed in Fig. 9. It is likely that the grafting reaction with itaconic anhydride in the Brabender

mixer causes unwanted incorporation of particles that act as nucleating agents for PLLA formulations. In fact, after melt processing commercial PLLA displays a much faster crystallization rate (c-PLLA$_{Pr}$ *vs.* c-PLLA plots). Crystallization rate data of c-PLLA$_{Pr}$ and PLLA-IAH overlap within experimental uncertainty, probing not only that the faster crystallization rate of PLLA-IAH compared to c-PLLA is due to melt processing, but also that PLLA-IAH can be used as reference to compare the effect of blending and grafting on crystallization kinetics.

The varied nucleation density caused by melt processing is revealed by optical microscopy analysis. The optical micrographs of PLLA-IAH prepared by Brabender mixing and of PLLA-g-PLLA$_{4k}$, both dissolved in chloroform to attain cast film, are compared in Fig. 10 to c-PLLA film attained by casting only. The micrographs refer to samples isothermally crystallized at 140 °C. A much higher nucleation density is obvious in the melt-processed samples, which causes the faster crystallization of the reacted polymer seen in Figs. 7–9.

The isothermal spherulite growth rates (G) of PLLA grafted with IAH, plain, blended with OH-terminated oligomer, and grafted with same oligomer, are presented in Fig. 11. G values are limited to $T_c \geq 115$ °C, as at lower temperatures the very high nucleation density complicates the attainment of reliable data. Experimental data are compared to spherulite growth rates of pristine c-PLLA, taken from Ref. [30], and with the same polymer after melt processing (c-PLLA$_{Pr}$). G data of both c-PLLA and c-PLLA$_{Pr}$ overlap, within experimental uncertainty, with G values of PLLA grafted with itaconic anhydride. Not only this confirms that the much faster crystallization rate of PLLA containing anhydride units detailed above, is caused by the enhanced nucleation, but provides the additional information that anhydride units randomly dispersed in the PLLA chains do not sizably disturb growth of PLLA crystals. Conversely, a significant increase in spherulite growth rate is observed in the blended formulation, which is even more marked in the copolymer.

As demonstrated in Ref. [30], in the blended formulation the stereoregular and more mobile entangled short chains of the OH-terminated oligomer start to crystallize at a higher temperature upon cooling, or in a shorter time upon isothermal crystallization, compared to the commercial PLLA of low stereoregularity and high molar mass. These crystals act as nuclei for the growth of PLLA crystals that contain both blend components which, in turn, is also facilitated by the presence of short chains. It can be hypothesized that a similar nucleation mechanism occurs in the graft copolymer, with an initial crystallization of the highly stereoregular side chains, whose crystallization kinetics is higher than that of the chain backbone, since the latter contains D-isomer units that act as chain defects interfering with crystal ordering. After primary nucleation, also a faster spherulite growth is observed, higher in the case of graft copolymer. Both increases can be rationalized taking into account that addition of short PLLA chains results in a lower T_g, especially in the blends, which facilitates transport of

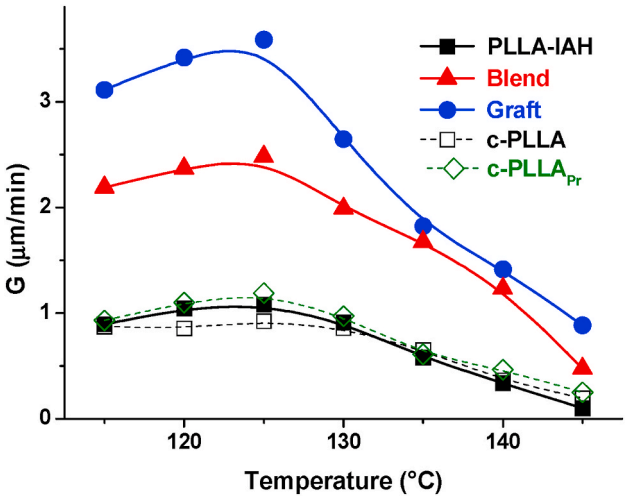

Fig. 11. Spherulite growth rates of PLLA formulations.

crystallizable chains in the melt across the liquid–solid interface, due to the higher chain mobility at parity of temperature. However, the increase in G is even more marked in the graft copolymer than in the blend, which suggests that additional effects need to be taken into account.

For long polymer molecules, the rate determining step of crystal growth has been named 'molecular nucleation' [53]: when a new polymer molecule is added to a crystal, first a small part of it nucleates on the growing substrate, then the remaining part of the chain is drawn from the entangled melt [54]. For both blend and graft copolymer, crystallization is initiated by the short stereoregular sequences. In the blend, once crystal nuclei made of stereoregular oligomers are developed, each long PLLA chain must attach to growing crystals (the 'molecular nucleation') before further chain ordering can lead to crystal growth. If in the graft copolymer the crystal nuclei are made of the short side chains, chemically bonded to the long PLLA backbones, the latter are already attached to the crystal surface, hence not need the molecular nucleation step for the subsequent crystal growth. This results in a faster crystal growth, as shown in Fig. 11, even faster than in the blend, at parity of T_g.

In other words, the synthesis of a graft copolymer with a well-defined length and amount of side chains by means of a tailored chemistry can provide an efficient way to attain a faster crystallization rate of PLLA, even higher than that attainable for a blend with the same nominal composition.

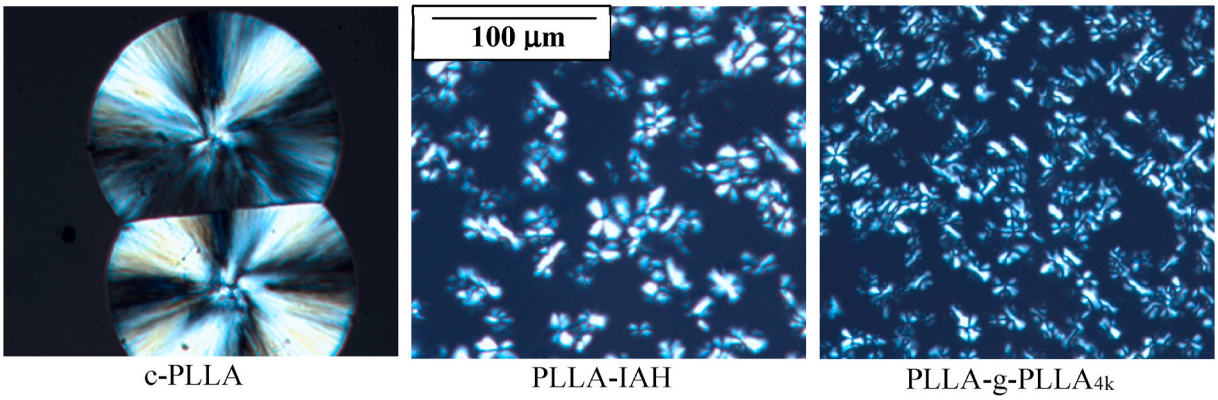

Fig. 10. Optical micrographs (crossed polars) of PLLA formulations during isothermal crystallization at 140 °C.

4. Conclusions

A PLLA with a tailored amount and length of side branches randomly distributed along the main chain was synthesized by radical functionalization with IAH and subsequent coupling with short and optically pure PLLA chains able to enhance crystallization rate. The functionalization degree, determined by UV–vis spectroscopy is 0.5 wt%. The optically pure $PLLA_{4k}$ branches were introduced via nucleophilic attack to the IAH and the decrease in intrinsic viscosity combined with a deviation from linearity for high molecular weight in the Mark-Houwink plot of the graft copolymer proved the presence of branching, with an average value of one branch every 240 repeating units, randomly distributed along the PLLA chain.

Chain functionalization with IAH does not sizably vary the thermal properties of the polymer, nor the crystal growth rate, and the only measurable effect of an enhanced nucleation rate is due to unwanted incorporation of impurities upon processing. Compared to a binary blend with the same nominal composition, the graft copolymer displays a higher spherulite growth rate, which was rationalized in terms of molecular nucleation. The latter is a rate-limiting step in polymer crystallization, which is not needed in the copolymer, where the optically pure short side chains that crystallize earlier act as molecular nuclei for the subsequent attachment of the main chain backbone to the crystals.

The enhancement of crystallization kinetics of poly (L-lactic acid) by copolymerization with optically pure branches has been demonstrated to date only for the chain architecture and composition detailed in this manuscript, i.e. for a graft copolymer made of side chains of $M_n = 4$ kDa randomly attached to a main chain on average every 240 repeating units. It is likely that crystallization rate of PLLA may be further improved beyond the results detailed here, by proper variation of side chains, in terms of chain length, density and composition. Furthermore, since the glass transition is only barely affected by chain architecture and composition, even faster crystallization rate can be attained by adding specific components to the formulation, i.e. by addition of plasticizers, beyond other specific additives like nucleating agents, paving a path to overcome one the main drawbacks of PLLA that have limited so far its wider commercial exploitation.

Declaration of competing interest

The authors declare that they have no known competing financial interests or personal relationships that could have appeared to influence the work reported in this paper.

Acknowledgements

The authors wish to thank Total Corbion for kindly providing PLLA and LLA, as well as Dr. Salvatore Mallardo (IPCB-CNR) for the essential assistance in the use of Rheocord.

References

[1] M.L. Di Lorenzo, R. Androsch, Synthesis, structure and properties of poly (lactic acid), Adv. Polym. Sci. 279 (2018), https://doi.org/10.1007/978-3-319-64230-7. Springer, Cham.
[2] M.L. Di Lorenzo, R. Androsch, Industrial applications of poly(lactic acid), Adv. Polym. Sci. 282 (2018), https://doi.org/10.1007/978-3-319-75459-8. Springer, Cham.
[3] R. Mehta, V. Kumar, H. Bhunia, S.N. Upadhyay, Synthesis of poly(lactic acid): a review, J. Macromol. Sci. Polym. Rev. (2005), https://doi.org/10.1080/15321790500304148.
[4] J. Tan, M.A. Abdel-Rahman, K. Sonomoto, Biorefinery-based lactic acid fermentation: microbial production of pure monomer product, in: M.L. Di Lorenzo, R. Androsch (Eds.), Synthesis, Structure and Properties of Poly(lactic Acid). Adv. Polym. Sci. 279, Springer, Cham, 2017, pp. 27–66, https://doi.org/10.1007/12_2016_11.
[5] J.A. Byers, A.B. Biernesser, K.R. Delle Chiaie, A. Kaur, J.A. Kehl, Catalytic systems for the production of poly(lactic acid), in: M.L. Di Lorenzo, R. Androsch (Eds.), Synthesis, Structure and Properties of Poly(lactic Acid). Adv. Polym. Sci. 279, Springer, Cham, 2017, pp. 67–118, https://doi.org/10.1007/12_2017_20.
[6] M.L. Di Lorenzo, P. Rubino, R. Luijkx, M. Hélou, Influence of chain structure on crystal polymorphism of poly(lactic acid). Part 1: effect of optical purity of the monomer, Colloid Polym. Sci. (2014), https://doi.org/10.1007/s00396-013-3081-z.
[7] M.L. Di Lorenzo, R. Androsch, Stability and reorganization of α'-crystals in random L/D-Lactide copolymers, Macromol. Chem. Phys. (2016), https://doi.org/10.1002/macp.201600073.
[8] M.L. Di Lorenzo, R. Androsch, Influence of α′-/α-crystal polymorphism on properties of poly(L-lactic acid), Polym. Int. (2019), https://doi.org/10.1002/pi.5707.
[9] Y. Wang, Y. Tashiro, K. Sonomoto, Fermentative production of lactic acid from renewable materials: recent achievements, prospects, and limits, J. Biosci. Bioeng. (2015), https://doi.org/10.1016/j.jbiosc.2014.06.003.
[10] Y. Di, S. Iannace, E. Di Maio, L. Nicolais, Reactively modified poly (lactic acid): properties and foam processing, Macromol. Mater. Eng. (2005), https://doi.org/10.1002/mame.200500115.
[11] D.C. Li, T. Liu, L. Zhao, X.S. Lian, W.K. Yuan, Foaming of poly(lactic acid) based on its nonisothermal crystallization behavior under compressed carbon dioxide, Ind. Eng. Chem. Res. 50 (2011) 1997–2007, https://doi.org/10.1021/ie101723g.
[12] M. Nofar, C.B. Park, Poly (lactic acid) foaming, Prog. Polym. Sci. 39 (2014) 1721–1741, https://doi.org/10.1016/j.progpolymsci.2014.04.001.
[13] S. Iannace, L. Sorrentino, E. Di Maio, Biodegradable biomedical foam scaffolds, in: Biomed. Foam. Tissue Eng. Appl., 2014, https://doi.org/10.1533/9780857097033.1.163.
[14] R. Androsch, M.L. Di Lorenzo, C. Schick, Crystal nucleation in random L/D-lactide copolymers, Eur. Polym. J. (2016), https://doi.org/10.1016/j.eurpolymj.2016.01.020.
[15] M.L. Di Lorenzo, R. Androsch, Crystallization of Poly(lactic acid), in: Biodegradable Polyesters, John Wiley & Sons, Ltd, 2015, pp. 109–130, https://doi.org/10.1002/9783527656950.ch5.
[16] R. Androsch, M.L. Di Lorenzo, C. Schick, Kinetics of nucleation and growth of crystals of poly(L-lactic) acid, in: Synthesis, Structure and Properties of Poly(lactic Acid), Springer, 2018.
[17] W. Zeng, J. Wang, Z. Feng, J.-Y. Dong, S. Yan, Morphologies of long chain branched isotactic polypropylene crystallized from melt, Colloid Polym. Sci. 284 (2005) 322–326.
[18] J. Tian, W. Yu, C. Zhou, Crystallization behaviors of linear and long chain branched polypropylene, J. Appl. Polym. Sci. 104 (2007) 3592–3600.
[19] J. Tian, W. Yu, C. Zhou, Crystallization kinetics of linear and long-chain branched polypropylene, J. Macromol. Sci. Part B. 45 (2006) 969–985.
[20] J. Liu, S. Zhang, L. Zhang, Y. Bai, Crystallization behavior of long-chain branching polylactide, Ind. Eng. Chem. Res. 51 (2012) 13670–13679.
[21] C. Zhao, D. Wu, N.A.N. Huang, H. Zhao, Crystallization and thermal properties of PLLA comb polymer, J. Polym. Sci., Part B: Polym. Phys. 46 (2008) 589–598.
[22] H. Tsuji, T. Miyase, Y. Tezuka, S.K. Saha, Physical properties, crystallization, and spherulite growth of linear and 3-arm poly (L-lactide) s, Biomacromolecules 6 (2005) 244–254.
[23] Q. Hao, F. Li, Q. Li, Y. Li, L. Jia, J. Yang, Q. Fang, A. Cao, Preparation and crystallization kinetics of new structurally well-defined star-shaped biodegradable poly (L-lactide) s initiated with diverse natural sugar alcohols, Biomacromolecules 6 (2005) 2236–2247.
[24] J.R. Dorgan, J.S. Williams, D.N. Lewis, Melt rheology of poly(lactic acid): entanglement and chain architecture effects, J. Rheol. (1999), https://doi.org/10.1122/1.551041.
[25] N. Najafi, M.-C. Heuzey, P. Carreau, D. Therriault, Quiescent and shear-induced crystallization of linear and branched polylactides, Rheol. Acta 54 (2015) 831–845.
[26] H. Tsuji, Quiescent crystallization of poly (lactic acid) and its copolymers-based materials, Therm. Prop. Bio-Based Polym. (2019) 37–86.
[27] G. Gorrasi, R. Pantani, Hydrolysis and biodegradation of poly(lactic acid), in: M. L. Di Lorenzo, R. Androsch (Eds.), Synthesis, Structure and Properties of Poly(lactic Acid). Adv. Polym. Sci. 279, Springer, Cham, 2017, pp. 119–151, https://doi.org/10.1007/12_2016_12.
[28] N. Burgos, D. Tolaguera, S. Fiori, A. Jiménez, Synthesis and characterization of lactic acid oligomers: evaluation of performance as poly (lactic acid) plasticizers, J. Polym. Environ. 22 (2014) 227–235.
[29] R. Avolio, R. Castaldo, G. Gentile, V. Ambrogi, S. Fiori, M. Avella, M. Cocca, M. E. Errico, Plasticization of poly (lactic acid) through blending with oligomers of lactic acid: effect of the physical aging on properties, Eur. Polym. J. 66 (2015) 533–542.
[30] M.L. Di Lorenzo, R. Androsch, Accelerated crystallization of high molar mass poly (L/D-lactic acid) by blending with low molar mass poly (l-lactic acid), Eur. Polym. J. 100 (2018) 172–177.
[31] J. Pan, Y. Wang, S. Qin, B. Zhang, Y. Luo, Grafting reaction of poly (D, L) lactic acid with maleic anhydride and hexanediamine to introduce more reactive groups in its bulk, J. Biomed. Mater. Res. Part B Appl. Biomater. An Off. J. Soc. Biomater. Japanese Soc. Biomater. Aust. Soc. Biomater. Korean Soc. Biomater. 74 (2005) 476–480.
[32] D. Carlson, L. Nie, R. Narayan, P. Dubois, Maleation of polylactide (PLA) by reactive extrusion, J. Appl. Polym. Sci. 72 (1999) 477–485.
[33] S.W. Hwang, S.B. Lee, C.K. Lee, J.Y. Lee, J.K. Shim, S.E.M. Selke, H. Soto-Valdez, L. Matuana, M. Rubino, R. Auras, Grafting of maleic anhydride on poly (L-lactic acid). Effects on physical and mechanical properties, Polym. Test. 31 (2012) 333–344.

[34] J. Petruš, F. Kučera, I. Chamradová, J. Jančář, Real-time monitoring of radical grafting of poly (lactic acid) with itaconic anhydride in melt, Eur. Polym. J. 103 (2018) 378–389.
[35] J. Petruš, F. Kučera, J. Petrůj, Post-polymerization modification of poly (lactic acid) via radical grafting with itaconic anhydride, Eur. Polym. J. 77 (2016) 16–30.
[36] Luminy LX175 Product Data Sheet, revised 1 Sept 2017., (n.d.).
[37] M.N. Collins, C. Birkinshaw, Physical properties of crosslinked hyaluronic acid hydrogels, J. Mater. Sci. Mater. Med. 19 (2008) 3335–3343, https://doi.org/10.1007/s10856-008-3476-4.
[38] X. Jiang, J. Zhou, Y. Zhou, H. Sun, J. Xu, F. Feng, W. Qu, Convenient method of synthesizing aryloxyalkyl esters from phenolic esters using halogenated alcohols, Molecules 23 (2018) 1715, https://doi.org/10.3390/molecules23071715.
[39] K. Suganuma, K. Horiuchi, H. Matsuda, H.N. Cheng, A. Aoki, T. Asakura, NMR analysis and chemical shift calculations of poly(lactic acid) dimer model compounds with different tacticities, Polym. J. 44 (2012) 838–844, https://doi.org/10.1038/pj.2012.106.
[40] W. Liu, T. Liu, T. Liu, T. Liu, J. Xin, W.C. Hiscox, H. Liu, L. Liu, J. Zhang, Improving grafting efficiency of dicarboxylic anhydride monomer on polylactic acid by manipulating monomer structure and using comonomer and reducing agent, Ind. Eng. Chem. Res. 56 (2017) 3920–3927, https://doi.org/10.1021/acs.iecr.6b05051.
[41] Y. Cui, M. Wang, L. Chen, G. Qian, Synthesis and spectroscopic characterization of an alkoxysilane dye containing CI Disperse Red 1, Dye. Pigment 62 (2004) 43–47.
[42] M. Kurata, M. Abe, M. Iwama, M. Matsushima, Randomly branched polymers. I. Hydrodynamic properties, Polym. J. 3 (1972) 729–738.
[43] P.M. Wood-Adams, J.M. Dealy, A.W. Degroot, O.D. Redwine, Effect of molecular structure on the linear viscoelastic behavior of polyethylene, Macromolecules 33 (2000) 7489–7499.
[44] B. Wunderlich, Thermal Analysis, Academic Press, Inc., New York, 1990.
[45] O. Martin, L. Avérous, Poly(lactic acid): plasticization and properties of biodegradable multiphase systems, Polymer 42 (2001) 6209–6219, https://doi.org/10.1016/S0032-3861(01)00086-6.
[46] J. Ambrosio-Martín, M.J. Fabra, A. Lopez-Rubio, J.M. Lagaron, An effect of lactic acid oligomers on the barrier properties of polylactide, J. Mater. Sci. 49 (2014) 2975–2986.
[47] R.N. Darie-Niţə, C. Vasile, A. Irimia, R. Lipşa, M. Râpə, Evaluation of some eco-friendly plasticizers for PLA films processing, J. Appl. Polym. Sci. (2016), https://doi.org/10.1002/app.43223.
[48] M.K. Fehri, C. Mugoni, P. Cinelli, I. Anguillesi, M.B. Coltelli, S. Fiori, M. Montorsi, A. Lazzeri, Composition Dependence of the Synergistic Effect of Nucleating Agent and Plasticizer in Poly (Lactic Acid): A Mixture Design Study, 2016.
[49] F. Cicogna, S. Coiai, C. De Monte, R. Spiniello, S. Fiori, M. Franceschi, F. Braca, P. Cinelli, S.M.K. Fehri, A. Lazzeri, Poly (lactic acid) plasticized with low-molecular-weight polyesters: structural, thermal and biodegradability features, Polym. Int. 66 (2017) 761–769.
[50] Y. Tsukahara, K. Tsutsumi, Y. Okamoto, On some bulk properties of poly (macromonomer)s, Makromol. Chem. Rapid Commun. 13 (1992) 409–413, https://doi.org/10.1002/marc.1992.030130902.
[51] D. Vlassopoulos, G. Fytas, B. Loppinet, F. Isel, P. Lutz, H. Benoit, Polymacromonomers: structure and dynamics in nondilute solutions, melts, and mixtures, Macromolecules 33 (2000) 5960–5969.
[52] F. Auriemma, C. De Rosa, R. Di Girolamo, A. Silvestre, A.M. Anderson-Wile, G. W. Coates, Small angle x-ray scattering investigation of norbornene-terminated syndiotactic polypropylene and corresponding comb-like poly (macromonomer), J. Phys. Chem. B 117 (2013) 10320–10333.
[53] B. Wunderlich, Molecular nucleation and segregation, Faraday Discuss. Chem. Soc. 68 (1979) 239–243.
[54] B. Wunderlich, A. Mehta, Macromolecular nucleation, J. Polym. Sci., Polym. Phys. Ed. 12 (1974) 255–263.